Substorm-induced energetic electron precipitation: Impact on atmospheric chemistry

A. Seppälä[1], M. A. Clilverd[2], M. J. Beharrell[3], C. J Rodger[4], P. T. Verronen[1], M. E. Andersson[1], and D. A. Newnham[2]

Corresponding author: A. Seppälä, Finnish Meteorological Institute, Helsinki, Finland. (annika.seppala@fmi.fi)

[1]Finnish Meteorological Institute, Helsinki, Finland.

[2]British Antarctic Survey/NERC, Cambridge, UK

[3]Physics Department, Lancaster University, Lancaster, UK

[4]Physics Department, Otago University, Dunedin, New Zealand

Magnetospheric substorms drive energetic electron precipitation into the Earth's atmosphere. We use the output from a substorm model to describe electron precipitation forcing of the atmosphere during an active substorm period in April-May 2007. We provide the first estimate of substorm impact on the neutral composition of the polar middle atmosphere. Model simulations show that the enhanced ionization from a series of substorms leads to an estimated ozone loss of 5–50% in the mesospheric column depending on season. This is similar in scale to small to medium solar proton events (SPEs). This effect on polar ozone balance is potentially more important on long time scales (months-years) than the impulsive but sporadic (few SPE/year vs. 3-4 substorms/day) effect of SPEs. Our results suggest that substorms should be considered an important source of energetic particle precipitation into the atmosphere and included in high-top chemistry-climate models.

1. Introduction

Magnetospheric substorms are short-lived reconfigurations of the geomagnetic field and result in energetic electron precipitation (EEP) into the atmosphere lasting several hours [*Akasofu*, 1981; *Cresswell-Moorcock et al.*, 2013]. Electron precipitation energies during substorms can occur from 20 keV to 1 MeV, although typically the range is 20-300 keV [*Beharrell et al.*, 2015]. During the substorm injection process electron precipitation is initially detected at L∼6 [*Cresswell-Moorcock et al.*, 2013], and expands equatorwards and polewards with time. In a comprehensive study *Cresswell-Moorcock et al.* [2013] found that a typical substorm precipitation region spans the range L= $4.6 - 14.5$ (62°-75° invariant latitude). From the initial injection region close to magnetic midnight, the ionospheric footprint of the substorm expands eastwards, over many hours of local time, with velocities associated with the drift rates of 50-300 keV electrons [*Berkey et al.*, 1974]. The annual substorm rate is typically 1250, ranging from ∼500/year during quiet geomagnetic years to ∼2200/year during active years [Rodger et al., J. Geophys. Res., revised September 2015].

EEP into the atmosphere generates odd nitrogen (NO_x = N + NO + NO_2) and odd hydrogen (HO_x = OH + HO_2) species [*Codrescu et al.*, 1997]. For electron energies of 20-300 keV the altitudes over which atmospheric ionisation occurs is 60-90 km [*Turunen et al.*, 2009; *Fang et al.*, 2010]. Both NO_x and HO_x take part in short- and long-term catalytic destruction of ozone, dependent on altitude, photolysis levels, and atmospheric transport conditions [*Jackman et al.*, 2008, 2009]. Impacts to middle atmosphere ozone by energetic particle precipitation (EPP) may show influences all the way to the surface [*Rozanov*

et al., 2005; *Seppälä et al.*, 2009]. To date no analysis has been undertaken of the impact of substorm electron precipitation on the chemical balance of the atmosphere. The impact on the atmosphere will depend on the electron fluxes involved, the longitude at which the injection took place, the substorm occurrence rate, and the duration of elevated substorm activity. *Beharrell et al.* [2015] developed a model of substorm precipitation incorporating all of these features, modelling a specific period of substorm activity in April-May 2007. The precipitating flux magnitudes were determined by matching the observed riometer absorption levels at Kilpisjärvi, Finland, and hence generating a time sequence of well characterised substorms over a period of five days.

In this study we utilise the precipitating flux output from the *Beharrell et al.* [2015] substorm model in order to describe the electron precipitation input into an atmospheric model (the Sodankylä Ion and neutral Chemistry model, SIC). We investigate if substorms can generate significant levels of NO_x and HO_x, and if they are important enough to the atmospheric ozone balance to be considered as relevant for inclusion in coupled chemistry-climate model studies. We consider the effect of a realistic sequence of substorm events and how the atmospheric response depends on season.

2. Model setup and particle ionization

The atmospheric impact simulations were made with the Sodankylä Ion and neutral Chemistry model [see *Verronen et al.*, 2005; *Turunen et al.*, 2009]. The SIC model (v6.11.1) is a 1-D model aimed at studying processes in the middle atmosphere and the lower ionosphere, between the altitudes of 20–150 km, with 1 km vertical resolution. The model solves the concentrations of 43 positive and 29 negative ions, and 16 neutral

constituents, with the background neutral atmosphere and temperatures taken from the empirical, solar activity dependent MSIS-E-90 model for each 5 min timestep. For a daily changing solar spectrum, the SIC model utilizes the empirical Solar Irradiance Platform [formerly SOLAR2000, *Tobiska and Bouwer*, 2006].

We ran the SIC model for a single location in the Northern Hemisphere auroral zone, located above Kilpisjärvi, Finland (69°N, 20°E, L∼6). This location and the initial timing (27 April - 6 May, 2007) of the simulation correspond to the substorm analysis presented in *Beharrell et al.* [2015].

Figure 1 shows how different geomagnetic activity indicators behaved during the substorm period under investigation (27 April - 6 May, 2007). The *Dst*-index which is a measure of the strength of the magnetospheric ring current and can be used to identify onsets of geomagnetic storms. The Auroral Electrojet (AE) index represents electric currents flowing in the auroral zone ionosphere and can be used to indicate individual substorm occurrence. No enhancements in solar protons occurred in this time. According to the *Dst*-index a geomagnetic storm began late on the 27 April, and continued until about 1 May. The rapidly varying AE-index suggests that the disturbed period contained many substorms. *Beharrell et al.* [2015] used the SuperMAG substorm list [*Newell and Gjerloev*, 2011] to identify the times of substorms during this initial disturbed period, at a rate of ∼15/day. This is higher than the average 3-4/day [*Cresswell-Moorcock et al.*, 2013], but not exceptional for geomagnetically active periods. Electron ionization rates (Figure 2) calculated from the electron precipitation flux [see *Beharrell et al.*, 2015, for details] are used as an input to the SIC model to calculate the atmospheric response.

These rates show that several individual substorms (*Beharrell et al.* identified 61 substorms) took place during the five day period, with the most intense ionization taking place during the peak times indicated by *AE* in Figure 1. Following the initial five days of substorm electron precipitation, the model simulations were extended for a further five days without any additional electron precipitation forcing to examine how the chemical changes developed after the storm period. As can be seen in Figure 1, during these latter five days (2-5 May) no major disturbances were detected in the activity indices.

3. Results

The simulated impact of the April-May 2007 substorm period on mesospheric ozone above Kilpisjärvi is presented in Figure 3. The main ozone loss occurs between the altitudes of about 70 and 85 km. Most of the ozone destruction is driven by reactions involving the HO_x family, with a smaller contribution from the NO_x family, and there is a clear diurnal cycle present [*Verronen et al.*, 2005]. The largest losses occur during times when the substorm frequency is also at its greatest, on 29–30 April, and peak at ∼50% at 80–82 km. After the substorm forcing finishes on the 1st of May, photolysis-driven ozone recovery to background levels occurs within about 2 days. These ozone changes are of similar magnitude to those reported for electron precipitation from the radiation belts [*Rodger et al.*, 2010], although that study considered lower geomagnetic latitudes.

As the EPP impact on atmospheric chemistry is known to strongly depend on sunlight [*Jackman et al.*, 2008], we performed two further simulations to estimate the seasonality of substorm impact on the atmosphere. We estimated the impact that the *Beharrell et al.* [2015] modeled substorms precipitating fluxes would have should they occur during the

Northern Hemisphere (NH) summer solstice (June). Next we repeated the experiment during NH winter solstice (December). Both simulations were set at Kilpisjärvi (69°N, 20°E).

Figure 4 shows the change in the ozone, HO_x and NO_x columns across a 20-km wide peak ionisation impact region during the original April-May substorm period (see Figure 3) in blue, summer solstice (NH, June) in red and winter solstice (NH, December) in yellow. For the winter solstice case, the peak ionization altitude (as seen in Figure 2) is slightly lower due to seasonal background neutral atmosphere changes, and the maximum impact region consequently shifts slightly down towards the stratopause (64–84 km for December vs 70–90 km for April-May and June). The April-May and the summer solstice substorm precipitation results in up to 10% loss in ozone (70–90 km column loss of 10^{13} 1/cm^2), but during winter the substorms result in up to 50% loss in the ozone partial column (64–84 km column loss of 10^{15} 1/cm^2, for direct comparison, in the 70–90 km column the winter loss is also 10^{15} 1/cm^2). During the winter period, the recovery takes longer than the other periods, with ozone losses still present at the end of the 10-day simulation period. The large seasonal differences in the ozone loss can be understood with the large change in solar zenith angle and the larger percentage HO_x change during winter [see *Jackman et al.*, 2008, and references therein]. The HO_x and NO_x columns show rapid changes in response to additional ionisation arising from the substorms. HO_x shows both the fast production during the substorms and swift loss after the ionization finishes. NO_x remains enhanced beyond the substorm period, with gradual recovery afterwards over several days in April and summer, whilst for winter the enhancements remain elevated even after the

end of the 10 day simulation period due to the lack of effective NO_x loss via photolysis in the polar night. The overall percentage enhancements in winter are smaller due to the larger seasonal mesospheric NO_x background densities, while the absolute increases are similar in all cases ($4 - 6 \times 10^{13}$ $1/cm^2$). Nevertheless, in winter the NO_x enhancements are still of the order of several hundred percent, with little change by the end of the 10 day period, unlike for April and summer when the NO_x levels are strongly influenced by loss through photolysis.

4. Discussion

We have presented the first simulated estimates for the impact of substorm driven electron precipitation on polar middle atmosphere chemical balance. Ionization rates calculated from the results of *Beharrell et al.* [2015] for a series of substorms taking place in April-May 2007 indicate additional ionization reaching as far down as ∼65km (Figure 2). Our model simulation suggest that this ionization would lead to a 30–60% ozone loss at 80 km, and 3–10% ozone loss in the 70–90 km sub-column (during equinox) over a period of several days, with the ozone balance rapidly recovering after the substorms end. Depending on season, we estimate that for the 20 km vertical layer experiencing the peak impact, the altitude of which also depends on season, ozone losses driven by the substorms will range from about 5% to up to 50%, similar in scale to the impacts from small to medium solar proton events [*Seppälä et al.*, 2005; *Jackman et al.*, 2011; *von Clarmann et. al.*, 2013], or energetic electron precipitation from the radiation belts [*Rodger et al.*, 2010; *Andersson et al.*, 2014]. These are accompanied by up to an order of magnitude enhancements in HO_x and NO_x concentrations depending on the season,

with HO_x increases largest in winter and NO_x in summer. NO_x enhancements (∼200-300%), along with ozone losses, are still present under winter conditions five days after the substorm forcing was turned off in the model. The simulated changes in HO_x, NO_x and O_3 are of a magnitude and duration which should be possible to detect from satellite and ground-based observations. The levels of NO_x enhancement and ozone loss are such that ground-based passive millimeter-wave radiometry [*Newnham et al.*, 2013] could, under optimal atmospheric observing conditions, be capable of detecting the chemical effect of individual, large substorms. Analysis of observational data for impacts of substorms on atmospheric chemistry is the next step of our study.

As substorms are estimated to be occuring on average 3-4 times a day [*Cresswell-Moorcock et al.*, 2013], the impact on high-latitude middle atmosphere ozone balance from the substorm driven ionization is potentially more important on long time scales than the impulsive but sporadic effect of SPEs, although the altitude range is more limited. Our results suggest that along with EEP from the radiation belts, substorms need to be considered as an important source of EPP into the atmosphere, part of the natural solar forcing into the atmosphere-climate system [*Seppälä et al.*, 2014]. Further work is needed to estimate the long term substorm ionization forcing and its variation over solar cycle, and longer, timescales. For the use in chemistry-climate models also the geographic coverage of EEP from substorms should be better estimated, with some of the possibilities using satellite observations demonstrated by *Cresswell-Moorcock et al.* [2013].

Acknowledgments. We would like to thank the geomagnetic data suppliers and the World Data Center for Geomagnetism, Kyoto, for making the *Dst* and *AE* index data

available via http://wdc.kugi.kyoto-u.ac.jp. We thank the Academy of Finland for supporting this research: AS was supported by the Finnish Academy Research Fellowship #258165 and #265005 (CLASP: Climate and Solar Particle Forcing) and PTV and MEA were supported through the project #276926 (SECTIC: Sun-Earth Connection Through Ion Chemistry). This work was also supported by the UK Natural Environmental Research Council (grant NE/J008125/1). The data supporting the analysis and conclusions are available from the corresponding author.

References

Akasofu, S. I. (1981), Energy coupling between the solar wind and the magnetosphere, *Space Sci. Rev.*, *28*(2), 121–190, doi:10.1007/BF00218810.

Andersson, M. E., P. T. Verronen, C. J. Rodger, M. A. Clilverd, and A. Seppälä (2014), Missing driver in the Sun–Earth connection from energetic electron precipitation impacts mesospheric ozone, *Nature Com.*, *5*, doi:10.1038/ncomms6197.

Beharrell, M. J., F. Honary, C. J. Rodger, and M. A. Clilverd (2015), Substorm-induced energetic electron precipitation: Morphology and prediction, *J. Geophys. Res.*, pp. 1–10, doi:10.1002/2014JA020632.

Berkey, F. T., V. M. Driatskiy, K. Henriksen, B. Hultqvist, D. H. Jelly, T. I. Shchuka, A. Theander, and J. Ylindemi (1974), A synoptic investigation of particle precipitation dynamics for 60 substorms in IQSY (1964-1965) and IASY (1969), *Planet. Space Sci.*, *22*(2), 255–307, doi:10.1016/0032-0633(74)90028-2.

Codrescu, M. V., T. J. Fuller-Rowell, R. Roble, and D. S. Evans (1997), Medium energy particle precipitation influences on the mesosphere and lower thermosphere, *J. Geophys.*

Res., *102*(A), 19,977–19,988, doi:10.1029/97JA01728.

Cresswell-Moorcock, K., C. J. Rodger, A. Kero, A. B. Collier, M. A. Clilverd, I. Häggström, and T. Pitkänen (2013), A reexamination of latitudinal limits of substorm-produced energetic electron precipitation, *J. Geophys. Res.*, *118*(1), 6694–6705, doi:10.1002/jgra.50598.

Fang, X., C. E. Randall, D. Lummerzheim, W. Wang, G. Lu, S. C. Solomon, and R. A. Frahm (2010), Parameterization of monoenergetic electron impact ionization, *Geophys. Res. Lett.*, *37*, L22106, doi:10.1029/2010GL045406.

Jackman, C. H., D. R. Marsh, F. M. Vitt, R. R. Garcia, E. L. Fleming, G. J. Labow, C. E. Randall, M. Lopez-Puertas, B. Funke, and T. von Clarmann (2008), Short- and medium-term atmospheric constituent effects of very large solar proton events, *Atmos. Chem. Phys.*, *8*(3), 765–785, doi:10.5194/acp-8-765-2008.

Jackman, C. H., D. R. Marsh, F. M. Vitt, R. R. Garcia, C. E. Randall, E. L. Fleming, and S. M. Frith (2009), Long-term middle atmospheric influence of very large solar proton events, *J. Geophys. Res.*, *114*, D11304, doi:10.1029/2008JD011415.

Jackman, C. H., D. R. Marsh, F. M. Vitt, R. G. Roble, C. E. Randall, P. F. Bernath, B. Funke, M. López-Puertas, S. Versick, and G. Stiller (2011), Northern Hemisphere atmospheric influence of the solar proton events and ground level enhancement in January 2005, *Atmos. Chem. Phys.*, *11*, 7715–7755, doi::10.5194/acp-11-6153-2011.

Newell, P. T., and J. W. Gjerloev (2011), Evaluation of SuperMAG auroral electrojet indices as indicators of substorms and auroral power, *J. Geophys. Res.*, *116*(A), A12211, doi:10.1029/2011JA016779.

Newnham, D. A., P. J. Espy, M. A. Clilverd, C. J. Rodger, A. Seppälä, D. J. Maxfield, P. Hartogh, C. Straub, K. Holmén, and R. B. Horne (2013), Observations of nitric oxide in the Antarctic middle atmosphere during recurrent geomagnetic storms, *J. Geophys. Res.*, *118*(1), 7874–7885, doi:10.1002/2013JA019056.

Rozanov, E. V., L. B. Callis, M. Schlesinger, F. Yang, N. Andronova, and V. A. Zubov (2005), Atmospheric response to NOy source due to energetic electron precipitation, *Geophys. Res. Lett.*, *32*, L14811, doi:10.1029/2005GL023041.

Rodger, C. J., M. A. Clilverd, A. Seppälä, N. R. Thomson, R. J. Gamble, M. Parrot, J.-A. Sauvaud, and T. Ulich (2010), Radiation belt electron precipitation due to geomagnetic storms: Significance to middle atmosphere ozone chemistry, *J. Geophys. Res.*, *115*, A11320, doi:10.1029/2010JA015599.

Seppälä, A. P. T. Verronen, V. F. Sofieva, J. Tamminen, E. Kyrölä, C. J. Rodger, and M. A. Clilverd (2005), Destruction of the tertiary ozone maximum during a solar proton event, *Geophys. Res. Lett.*, *33*, L07804, doi:10.1029/2005GL025571.

Seppälä, A., C. E. Randall, M. A. Clilverd, E. V. Rozanov, and C. J. Rodger (2009), Geomagnetic activity and polar surface air temperature variability, *J. Geophys. Res.*, *114*, A10312, doi:10.1029/2008JA014029.

Seppälä, A., K. Matthes, C. E. Randall, and I. A. Mironova (2014), What is the solar influence on climate? Overview of activities during CAWSES-II, *Prog. Earth Planet. Sci.*, *1*(1), 24, doi:10.1186/s40645-014-0024-3.

Tobiska, W. K., and S. Bouwer (2006), New developments in SOLAR2000 for space research and operations, *Adv. Space Res.*, *37*(2), 347–358, doi:10.1016/j.asr.2005.08.015.

Turunen, E., P. T. Verronen, A. Seppälä, C. J. Rodger, M. A. Clilverd, J. Tamminen, C. F. Enell, and T. Ulich (2009), Impact of different energies of precipitating particles on NOx generation in the middle and upper atmosphere during geomagnetic storms, *J. Atmos. Sol. Terr. Phys.*, *71*, 1176–1189, doi:10.1016/j.jastp.2008.07.005.

Verronen, P. T., A. Seppälä, M. A. Clilverd, C. J. Rodger, E. Kyrölä, C. F. Enell, T. Ulich, and E. Turunen (2005), Diurnal variation of ozone depletion during the October-November 2003 solar proton events, *J. Geophys. Res.*, *110*(A), doi: 10.1029/2004JA010932.

von Clarmann, T., B. Funke, M. López-Puertas, S. Kellmann, A. Linden, G. P. Stiller, C. H. Jackman, and V. L. Harvey (2013), The solar proton events in 2012 as observed by MIPAS, *Geophys. Res. Lett.*, *40*, 2339–2343, doi:10.1002/grl.50119.

Figure 1. Geomagnetic conditions during and following the substorm period of April–May 2007. Major disturbances correspond to negative values of *Dst*-index (black line) and geomagnetic storm onsets are indicated by a sudden, sharp drop (27-28 Apr). The Auroral Electrojet (*AE*, red line) responds to the individual substorm occurrences.

Figure 2. Ionisation in the atmosphere above Kilpisjärvi resulting from the energetic electron precipitation from the April-May 2007 substorms [*Beharrell et al.*, 2015].

Figure 3. Change in ozone density in April–May 2007 due to substorm driven electron precipitation as a percentage [%] change from the control simulation with no electron precipitation. Contour lines are shown for -5%, -10%, -15%,...-55% (white areas indicate losses smaller than 5%). The +-signs indicate the contour level corresponding to the given value. Times are local times for Kilpisjärvi (UTC+2h).

Figure 4. Change in the O_3, HO_x and NO_x columns in the mesospheric peak ionisation layer for the observed storm period (Apr, 70–90 km, blue), summer solstice (Jun, 70–90 km, red) and winter solstice (Dec, 64–84 km, yellow). The x-axis shows the time in days (UTC+2h) from the start of the substorm electron ionisation and the y-axis presents the change from the no-substorm forcing simulations as a percentage.

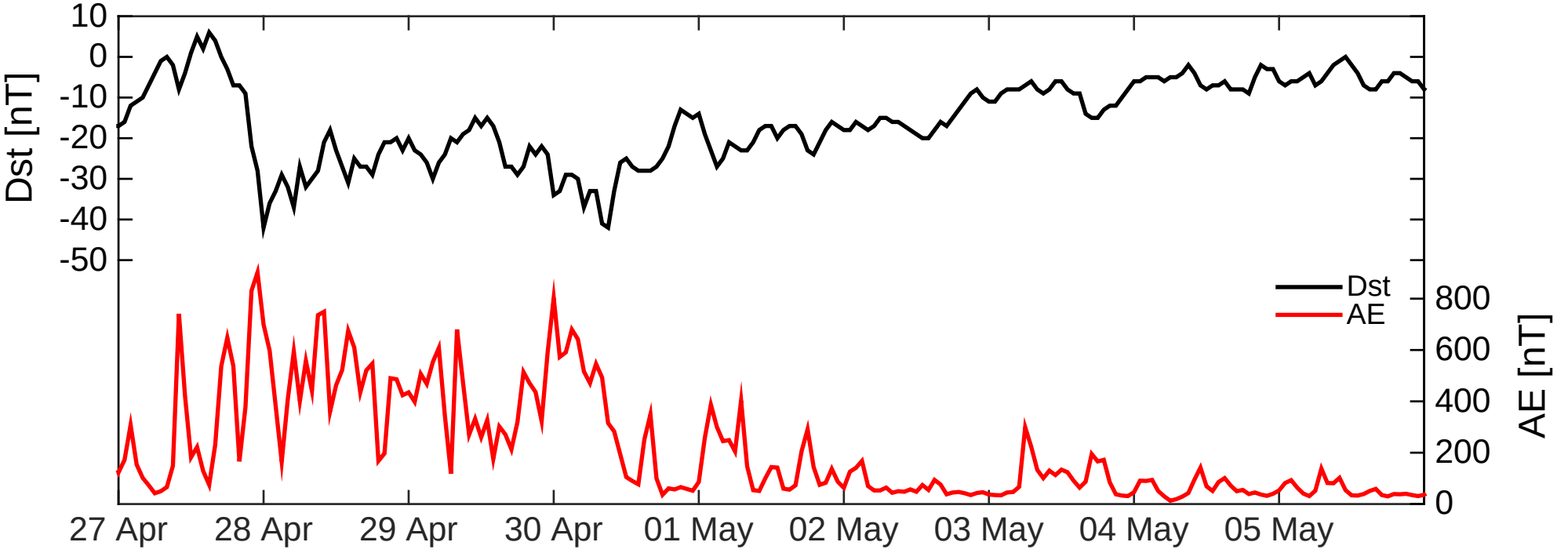
Dst [nT]
10
0
-10
-20
-30
-40
-50
Dst
AE
800
600
400
200
0
AE [nT]
27 Apr
28 Apr
29 Apr
30 Apr
01 May
02 May
03 May
04 May
05 May

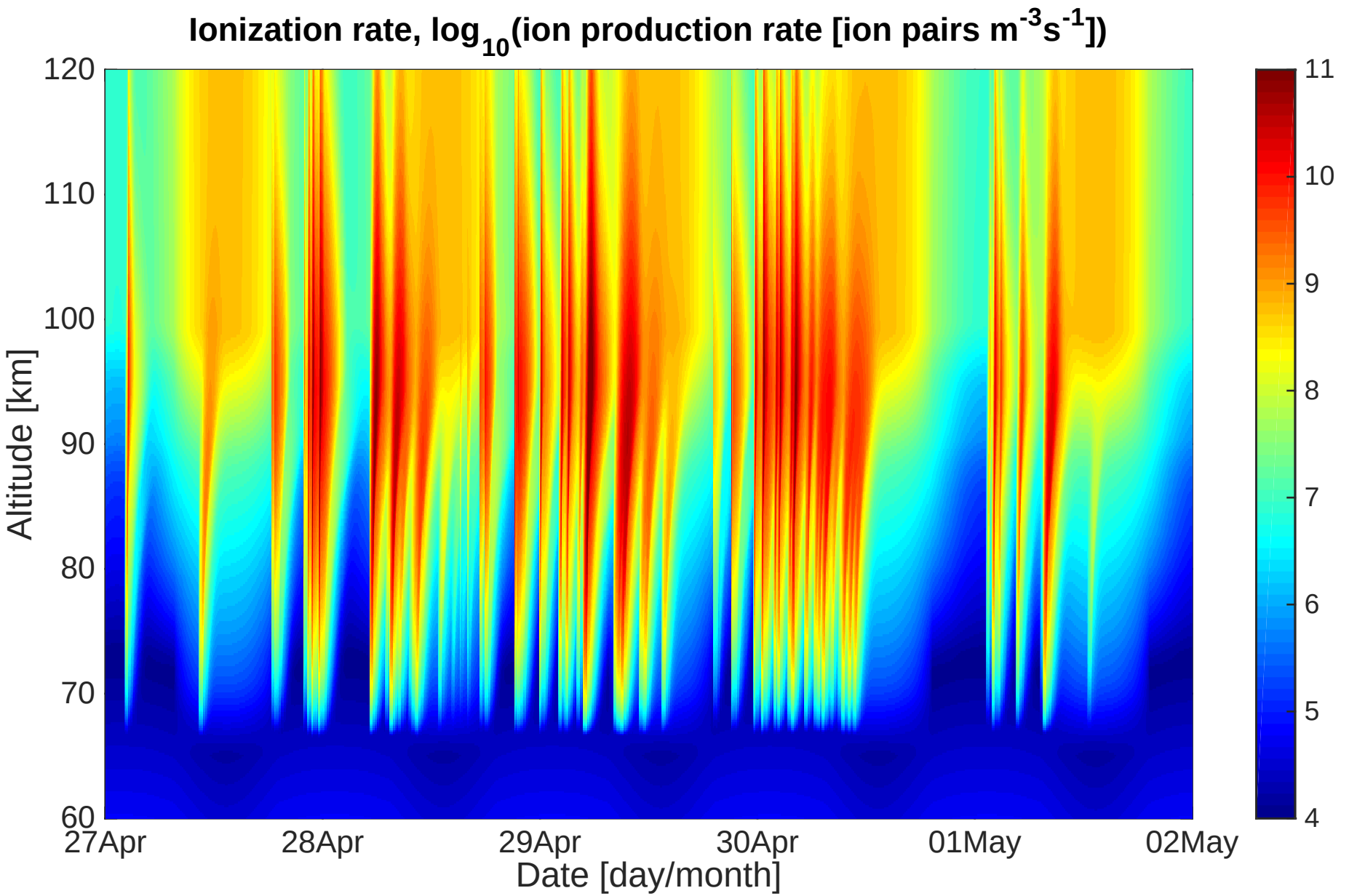
Ionization rate, log10(ion production rate [ion pairs m-3s-1])
120
110
100
90
80
70
60
Altitude [km]
27Apr
28Apr
29Apr
30Apr
01May
02May
Date [day/month]
11
10
9
8
7
6
5
4

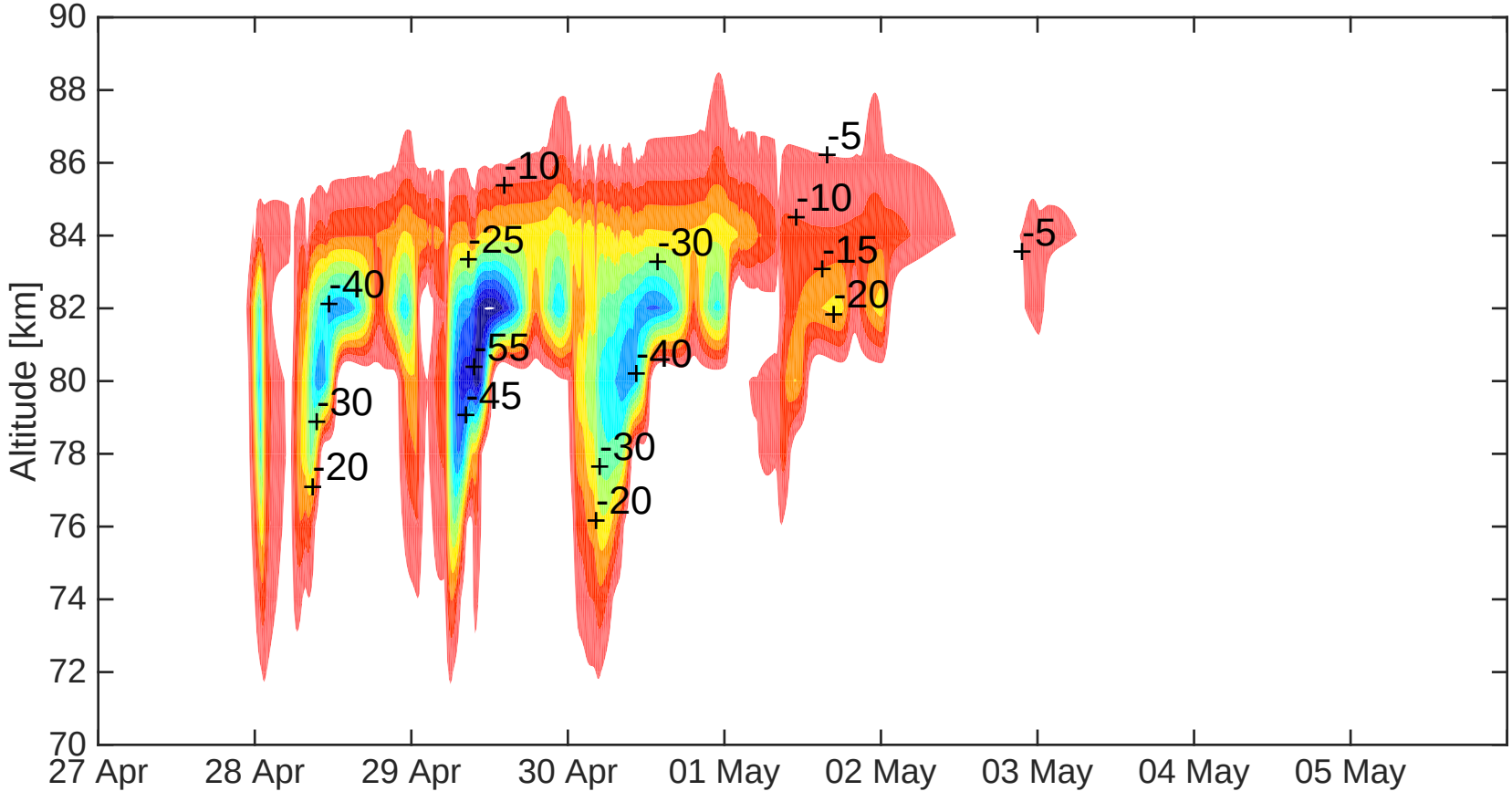
Altitude [km]
90
88
86
84
82
80
78
76
74
72
70
27 Apr
28 Apr
29 Apr
30 Apr
01 May
02 May
03 May
04 May
05 May
-10
-25
-40
-55
-30
-45
-20
-30
-40
-30
-20
-5
-10
-15
-20
-5

Change in O3 partial column

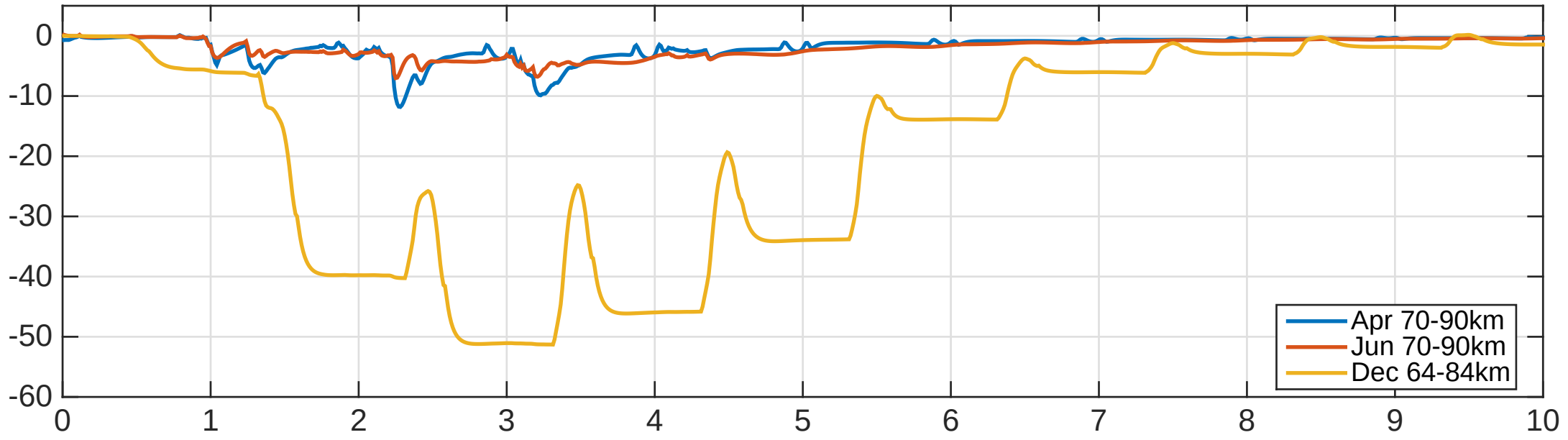

Change in HOx partial column

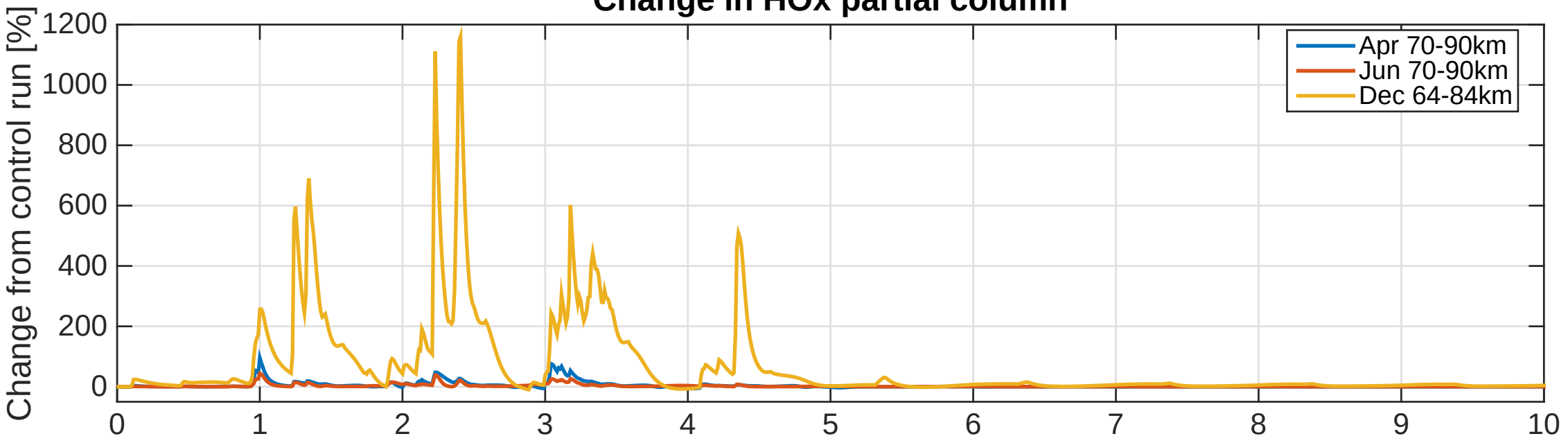

Change in NOx partial column